Mathematical Modeling of Monolithic Catalysts

Mathematical models are developed which account for simultaneous heat transfer, mass transfer, and chemical reaction in the oxidation of carbon monoxide over platinum containing monoliths. A two-dimensional model is shown to predict unusual behavior of the Nusselt number in the presence of rapid reaction. However, a simpler one-dimensional model is adequate for predicting monolith behavior.

ROLAND H. HECK
JAMES WEI
and
JAMES R. KATZER

Department of Chemical Engineering
University of Delaware
Newark, Delaware 19711

SCOPE

The oxidation of carbon monoxide and hydrocarbons is the principal reaction in an automobile catalytic converter. Half of the 1975 automobiles are equipped with monolithic converters in which platinum and palladium catalysts are deposited on the walls of a bundle of parallel ceramic tubes. The oxidation kinetics exhibits a negative reaction order with respect to carbon monoxide concentration, and the reactions are highly exothermic.

This paper describes a theoretical analysis of these unusual kinetics in monoliths. Steady state and transient temperature and concentration profiles are investigated, with numerical techniques used to solve the partial differential equations. The effects of inlet carbon monoxide concentration, inlet gas temperature, gas velocity, tube geometry, and diameter are investigated.

Young and Finlayson (1974) have shown that there is a significant difference between a one-dimensional model, where only axial gradients are considered, and a two-dimensional model, where both axial and radial gradients are considered. They have shown that in the two-dimensional model the Nusselt number shows an unusual behavior in the presence of rapid reactions. It would appear that the far more time consuming two-dimensional model must be used for the monolithic catalyst.

Overheating of the monolith in road use is often observed, to temperatures above the melting point of the ceramic material (about 1 400°C), even when the adiabatic flame temperature of the inlet gas is far below this temperature. An explanation for this phenomenon is needed.

CONCLUSIONS AND SIGNIFICANCE

This study confirmed the unusual behavior of the Nusselt number when the wall cools the gas in one section but heats the gas in a subsequent section. Despite this spectacular variation in the Nusselt number, the one- and two-dimensional models predict similar performance of the monolithic reactor (measured by the concentration profile). Thus, the simpler one-dimensional model is adequate for predicting monolith behavior during the crucial warm-up of an automobile from a cold start.

The monolithic reactor behavior is dominated by the position of the light-off point, where the catalytic wall temperature takes an upward leap, the wall concentration falls to zero, and the reaction becomes mass transport limited. In a typical 1975 automobile, with a rich exhaust during idle or deceleration, the position of the light-off point is dominated by the inlet gas temperature. At a sufficiently low inlet temperature, light-off does not occur, and the conversion is very low. For a very narrow range of intermediate inlet temperatures, light-off occurs in the tube; the conversion becomes increasing better as inlet temperature increases, and the light-off point moves towards the inlet. At a sufficiently high inlet temperature, the light-off occurs at the tube entrance, and conversion is completely controlled by mass transfer in the channel. The phenomenon of light-off is absent when the automobile is operating with a lean exhaust during acceleration and cruise.

The steady state temperature of the catalytic wall may exceed the adiabatic temperature of the gas if mass transport to the wall is much faster than heat transport from the wall. For molecules with Lewis number greater than one, such as hydrogen, the maximum wall temperature may be several times greater than the adiabatic flame temperature and may contribute to monolith destruction.

Monolithic catalysts are presently employed in 1975 and 1976 automobiles for the control of carbon monoxide and hydrocarbon emissions. These converters are unique chemical reactors and exhibit behavior different from that of conventional packed beds. They consist of an array of parallel channels with catalytic material deposited on the walls. Monoliths have been made with square, triangular, and sinusoidal channels.

One-dimensional models for prediction of packed-bed catalytic converter performance have been developed (Vardi and Biller, 1968; Kuo et al., 1971; Harned, 1973; Ferguson and Finlayson 1973). Young and Finlayson (1974) have developed and solved a two-dimensional model for a monolith using orthogonal collocation. They concluded that this more complicated model is necessary to predict monolith performance and showed that during certain operating transients, the solid temperature can exceed the maximum adiabatic gas temperature.

A two-dimensional model requires significantly more computer time than the simpler one-dimensional model. If the two can be made to agree reasonably well, the one-dimensional model is preferred. In this paper the simpler one-dimensional model is used to determine the effects of certain operating variables. A two-dimensional model is then developed and compared to this simpler model.

Roland H. Heck is with Mobil Research and Development, Paulsboro, New Jersey.

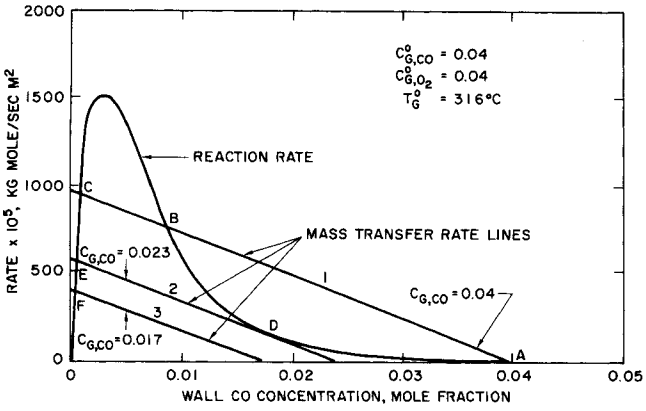

Fig. 1. Operating points for carbon monoxide oxidation in platinum containing monolith channel.

RESULTS AND DISCUSSION

One-Dimensional Model, Development

A mathematical model for reaction in a monolith must include the simultaneous processes of heat transfer, mass transfer, and chemical reaction. It was assumed that the gas-phase temperature, concentration, and velocity and the solid temperature were uniform across the monolith cross section. The rate of heat and mass transfer was assumed proportional to the difference between the gas and solid temperature and concentration; the proportionality factors are the heat and mass transfer coefficients. To simplify the analysis, axial conduction in the solid and in the gas were not included, and the reaction was assumed to take place only at the monolith surface. The model equations for the gas phase are

$$-\epsilon\bar{V}\rho_G C_{PG}\frac{\partial T_G}{\partial x} - hS\,(T_G - T_w) = \epsilon C_{PG}\rho_G\frac{\partial T_G}{\partial t} \quad (1)$$

$$-\epsilon\bar{V}\frac{\partial C_G}{\partial x} - k_m S\,(C_w - C_G) = \epsilon\frac{\partial C_G}{\partial t} \quad (2)$$

Heat and mass balances for the solid phase are

$$-r\Delta HS + hS\,(T_G - T_w) = \rho_w C_{Pw}\,(1-\epsilon)\frac{\partial T_w}{\partial t} \quad (3)$$

$$\frac{\rho_G k_m}{M_G}(C_G - C_w) = r \quad (4)$$

The kinetics for the oxidation of carbon monoxide over supported platinum given by Voltz et al. (1973) were used in this model:

$$r = \frac{k_r C C_{O_2}}{[1 + k_a C]^2} \quad (5)$$

$$k_r = k_r^o \exp\,[-E_r/R(T_w + 273)] \quad (6)$$

$$k_a = k_a^o \exp\,[-E_a/R(T_w + 273)] \quad (7)$$

The values of the constants used were

$$k_r^o = 4.14 \times 10^8 \quad \text{kg mole/m}^2\cdot\text{s}$$

$$k_a{}^o = 65.5$$

$$E_r/R = 12{,}600\ ^\circ\text{K}, \quad E_a/R = -961\ ^\circ\text{K}$$

Steady State Model

At steady state the time derivatives in Equations (1), (2), and (3) are equal to zero. If the equations are nondimensionalized, one obtains

$$\frac{dC_G}{dX^*} = \frac{Sh}{Le}(C_w - C_G) \quad (8)$$

$$\frac{dT_G}{dX^*} = Nu\,(T_w - T_G) \quad (9)$$

$$-r\Delta H = h\,(T_w - T_G) \quad (10)$$

$$r = \frac{\rho_G k_m}{M_G}(C_G - C_w) \quad (11)$$

where

$$X^* = \frac{4x/D}{Re\,Pr}$$

The dimensionless variable X^* is the Graetz number.

Combining Equations (10) and (11) with the equation for the adiabatic temperature rise

$$T_G = T_G{}^o + \frac{\Delta H C_G{}^o}{M_G C_{PG}}\left(1 - \frac{C_G}{C_G{}^o}\right) \quad (12)$$

we get

$$T_w = T_G{}^o + \left(1 - \frac{C_G}{C_G{}^o}\right)\Delta T_{AD} + \frac{Le\,Sh}{Nu}\left(\frac{C_G - C_w}{C_G{}^o}\right)T_{AD} \quad (13)$$

where

$$\Delta T_{AD} = \frac{\Delta H C_G{}^o}{M_G C_{PG}}$$

By using the analogy between heat and mass transfer, $Nu \cong Sh$, and the fact that for carbon monoxide $Le \cong 1$, Equation (13) is reduced to

$$T_w \cong T_G{}^o + \Delta T_{AD} = \left(1 - \frac{C_w}{C_G{}^o}\right) \quad (14)$$

Substitution of Equation (14) into Equations (6) and (7) allows the reaction rate to be calculated as a function of the wall carbon monoxide concentration for the adiabatic case.

Figure 1 shows the reaction rate as a function of C_w for an inlet temperature of 316°C and an inlet carbon monoxide concentration $C_G{}^o$ of 0.04. The heat of reaction ΔH included the heat of reaction of 1/3 mole of hydrogen for each mole of carbon monoxide, as suggested by Kuo et al. (1971).

As the gas moves down the tube, its temperature increases, and the carbon monoxide concentration decreases; both trends result in increased reaction rate. The rate reaches a maximum at $C_w = 0.003$ and then approaches zero as C_w approaches zero. The rate of mass transfer to the catalytic wall [Equation (11)] appears as a straight line with a slope of $(-\rho_G k_m)/(M_G)$ and an X intercept equal to C_G. The wall concentration corresponding to a given bulk gas concentration is given by the intersection of the reaction rate curve and mass transfer rate line. Figure 1 shows that from one to three solutions are possible. In the case with three solutions, the solution having a high wall concentration, point A, represents a stable solution resulting from an initially cold monolith. Solution *B* at $C_w \cong 0.01$ represents an unstable solution, and solution *C* at $C_w \cong 0.001$ represents the solution reached with an initially hot monolith. Since the cold start warm-up performance is of primary interest, the highest concentration, lowest temperature solution was used when multiple solutions existed.

For an initially cold monolith, the wall concentration at point A is approximately equal to the bulk concentration at the inlet. As the gas moves down the tube, the wall and bulk gas concentrations decrease smoothly until point D is reached. A further decrease in the bulk gas concentration results in a jump to solution E; this jump in the wall con-

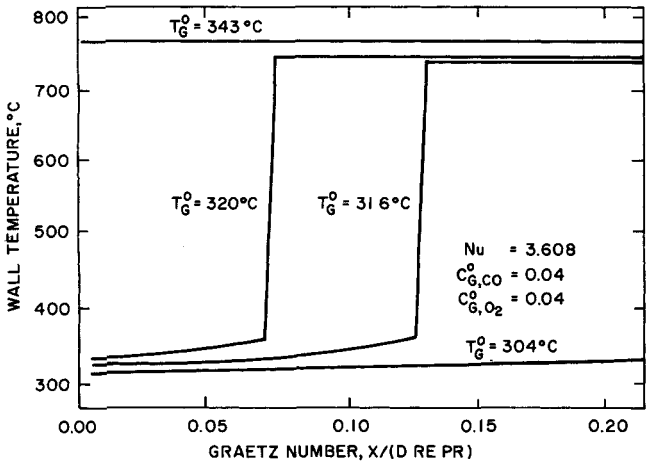

Fig. 2. Effect of inlet temperature on wall temperature profile in monolith channel.

TABLE 1. ASYMPTOTIC NUSSELT NUMBERS FROM ANALYTICAL SOLUTIONS* FOR FLOW IN DUCTS

Geometry of channel	Nu_H(1)	Nu_T(2)
○	4.364	3.657
□	3.608	2.976
△	3.111	2.470
≃	2.617	2.12

(1) Constant wall heat flux.
(2) Constant wall temperature.
* Shah and London, 1971.

centration and wall temperature is referred to as reaction light-off.

The equations were solved for several initial gas concentrations and temperatures by using the finite difference form of Equations (8) and (9). Equations (10) and (11) were solved by trial and error for each step. The step size was 0.0005, equivalent to about 0.0076 cm for a typical monolith.

One-Dimensional Model, Predictions

The results of the one-dimensional finite difference model for several inlet temperatures and for an asymptotic value of the Nusselt number characteristic of square channels are shown in Figure 2. These conditions are typical of 1975 automobiles operating with rich exhausts during idle or decelerations. For inlet gas temperatures below 304°C, the monolith temperature does not rise significantly above the inlet value, and conversion is minimal. For inlet gas temperatures between 304° and 343°C, the reaction lights-off at some point in the channel, and the wall temperature jumps to the adiabatic flame temperature. For inlet gas temperatures above 343°C, the monolith temperature is equal to the adiabatic flame temperature over its entire length. The transition temperature will depend on the values of the kinetic constants, but the behavior is general for most exothermic reactions, including carbon monoxide oxidation, over noble metals.

The values of the Nusselt number from analytical solutions for laminar flow in ducts of various shapes are given by Shah and London (1971) and are summarized in Table 1. These are the asymptotic values reached far from the tube inlet. The effect of channel geometry on the monolith wall temperature and on conversion is shown in Figures 3 and 4. A higher Nusselt number delays light-off and results in lower conversion at a given axial distance. When the entire tube is lit-off ($T > 343$°C), a higher Nusselt number results in higher conversion (Figure 5). Since the

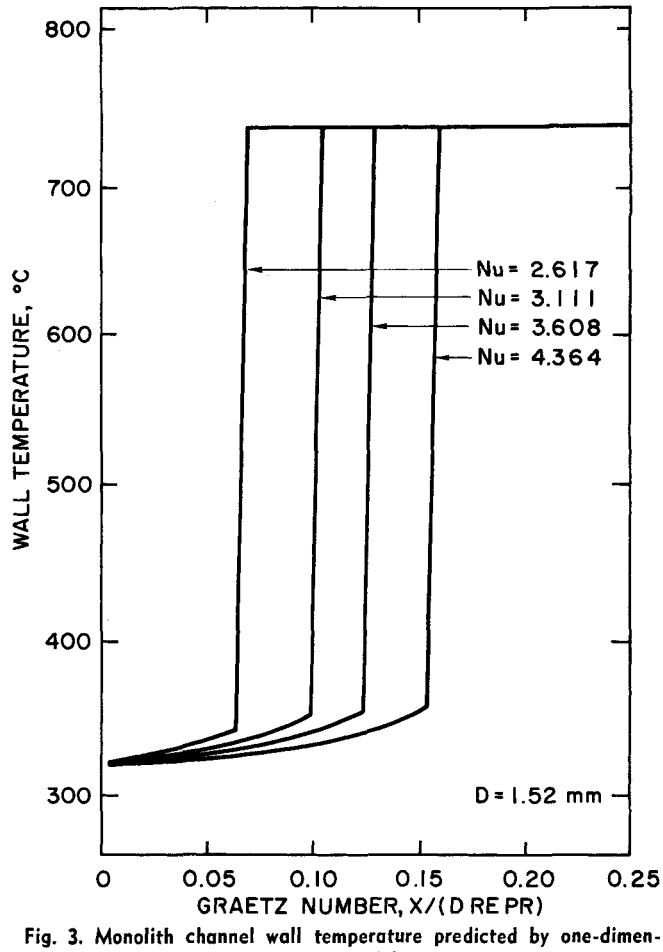

Fig. 3. Monolith channel wall temperature predicted by one-dimensional model.

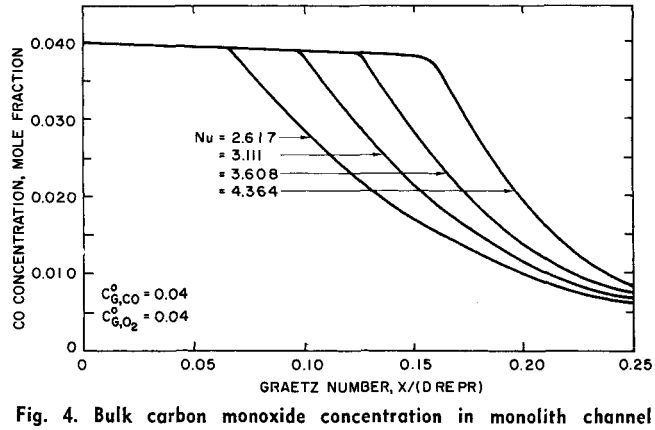

Fig. 4. Bulk carbon monoxide concentration in monolith channel predicted by one-dimensional model.

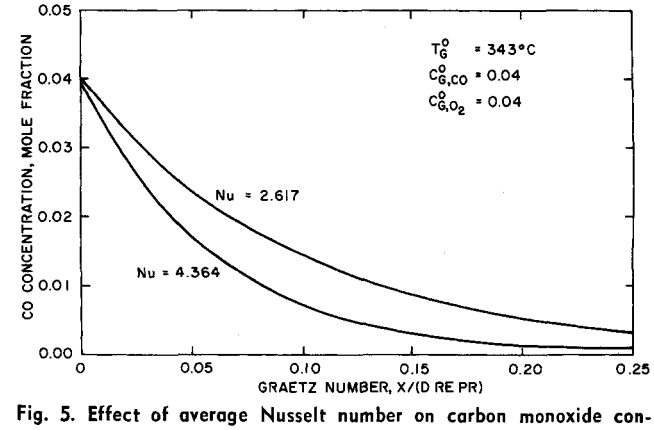

Fig. 5. Effect of average Nusselt number on carbon monoxide conversion according to one-dimensional model when light-off occurs at channel inlet.

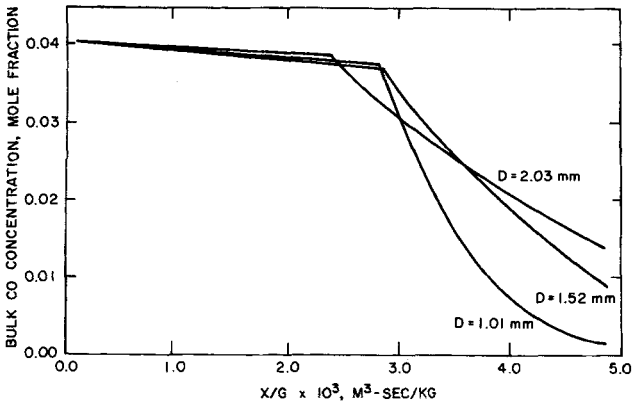

Fig. 6. Effect of channel diameter on carbon monoxide conversion.

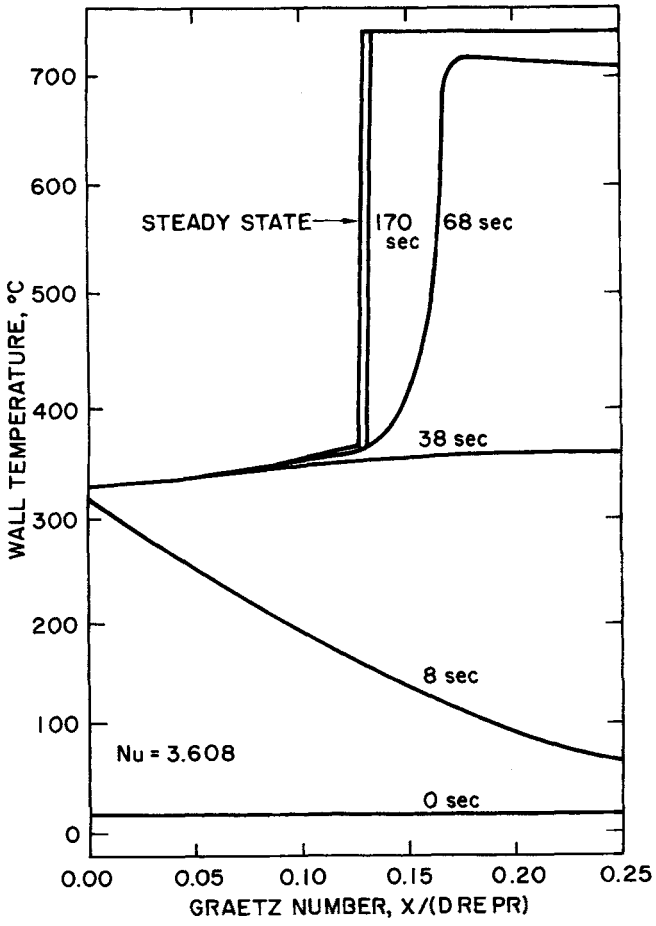

Fig. 7. Predicted transient temperatule profiles from one-dimensional model.

reaction is inhibited by carbon monoxide, a higher inlet carbon monoxide concentration delays light-off and thus reduces overall conversion. The slope of the mass transfer rate lines in Figure 1 is equal to $(-\rho_G K_m)/(M_G)$ or $(-\rho_G Sh\mathcal{D})/(M_G D)$. An increase in the Sherwood number or a decrease in D would make the mass transfer rate lines steeper and move the tangent point with the reaction rate curve to a lower value of wall and gas carbon monoxide concentration. When $(-\rho_G k_m/M_G)$ is greater than the maximum slope of $(-dr/dC_w)$, there is no tangent point, and the wall carbon monoxide concentration decreases continuously without the jump light-off.

Since the Graetz number is not a good distance parameter for comparing the effect of tube diameter because it contains the diameter squared in the denominator, X/G is used instead. Figure 6 shows that the largest diameter tube (2.03 mm) gives light-off at the shortest distance. However, for a given monolith length, overall conversion is highest for the smallest tube, except for tube lengths only slightly longer than that required for light-off.

When a 1975 automobile operates with lean exhausts during acceleration or cruise, carbon monoxide concentration is below 1% and so the kinetics is more nearly first order, and the adiabatic temperature rise is much lower. The reaction rate curve in Figure 1 would have a much lower maximum value, and the maximum rate value would be shifted towards a higher wall concentration. The phenomenon of light-off would be absent, and the exit concentration would be a smooth and continuous function of inlet temperature.

Transient Model, Predictions

The transient Equations (1) through (4) can be simplified by making the quasistatic approximation for the gas phase. This amounts to neglecting the accumulation of mass and energy in the gas phase, and thus $\partial T_w/\partial t$ is the only time derivative remaining. This approximation is justified because the thermal capacity of the solid is so large that it dominates the transient behavior of the system. The quasistatic assumption was made by Kuo et al. (1971) and Harned (1973) and is discussed at length by Ferguson and Finlayson (1974).

A typical result of the transient model is shown in Figure 7. The transience for this case is almost complete by 170 s.

Steady State Two-Dimensional Model, Development

In the two-dimensional model, a simple cylindrical channel was assumed to simplify the mathematics. The gas-phase temperature and concentration gradients in the radial as well as the axial direction were considered, and the rates of heat and mass transfer were calculated from these gradients. The basic equations of this model are

$$\frac{(1-R^2)}{2}\frac{\partial T_G}{\partial X^*} = \frac{1}{R}\frac{\partial}{\partial R}\left(R\frac{\partial T_G}{\partial R}\right) \tag{15}$$

$$\frac{(1-R^2)}{2}\frac{\partial C_G}{\partial X^*} = \frac{1}{LeR}\frac{\partial}{\partial R}\left(R\frac{\partial C_G}{\partial R}\right) \tag{16}$$

$$r\Delta H = \frac{2k_G}{D}\frac{\partial T_G}{\partial R}\bigg|_w \tag{17}$$

$$r = \frac{2\rho_G \mathcal{D}}{M_G D}\frac{\partial C_G}{\partial R}\bigg|_w \tag{18}$$

These equations were solved by a two-dimensional finite difference technique similar to that used by Kays (1955) for solution of the Graetz problem. Ten radial grid points were used together with an axial grid spacing of $\Delta X^* = 0.00025$.

Before the two-dimensional reaction problem was solved, the Graetz problem was solved for several unusual wall-flux boundary conditions to determine their effect on the Nusselt number. The Nusselt number is defined conventionally as

$$Nu = \frac{2\dfrac{\partial T}{\partial R}\bigg|_w}{(T_w - \overline{T}_G)} = \frac{2\dfrac{\partial T^*}{\partial R}\bigg|_w}{(T_w^* - \overline{T}_G^*)} \tag{19}$$

In the region of the tube where the reaction lights-off, the wall flux can be expected to rise rapidly and may jump discontinuously to a higher value. Figure 8 demonstrates the behavior of the Nusselt number in the regions driven by imposed rapidly rising wall flux. In case 1, the

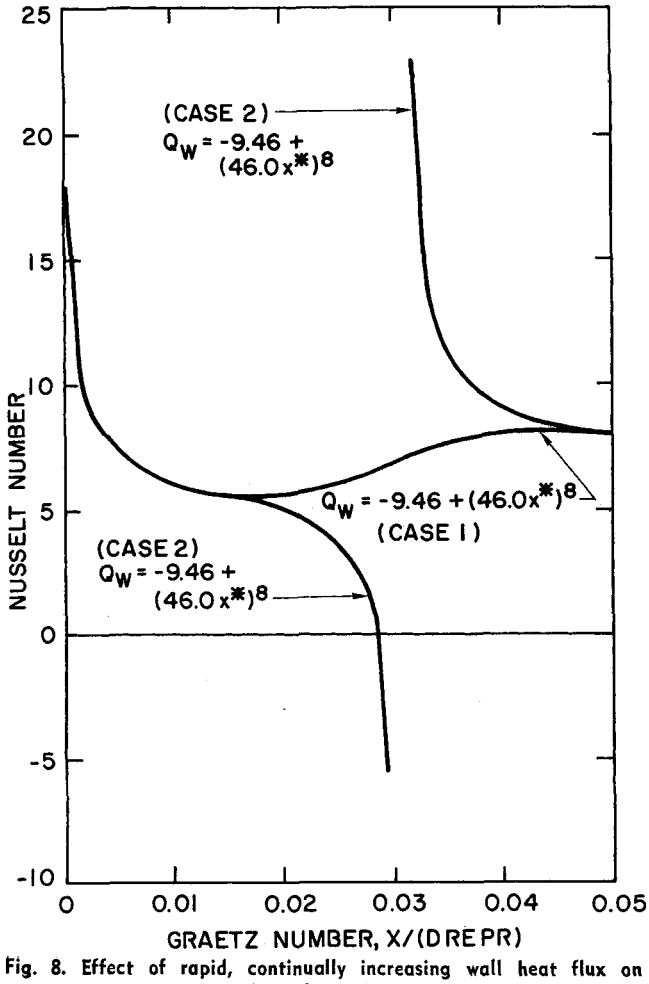

Fig. 8. Effect of rapid, continually increasing wall heat flux on Nusselt number.

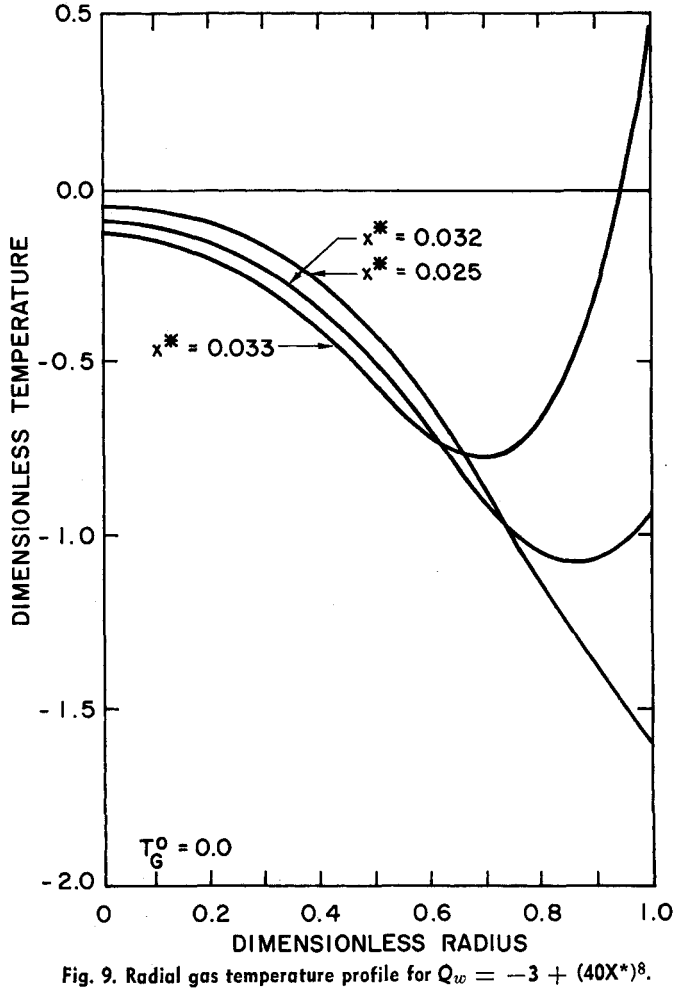

Fig. 9. Radial gas temperature profile for $Q_w = -3 + (40X^*)^8$.

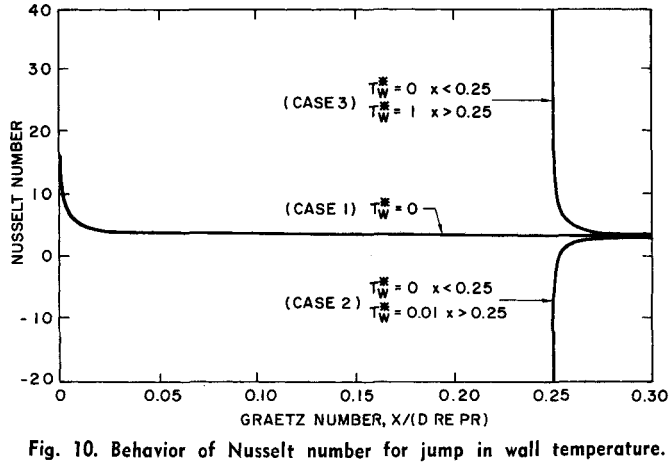

Fig. 10. Behavior of Nusselt number for jump in wall temperature.

wall flux is everywhere positive and rises rapidly in the region where $X^* = 0.025$. The Nusselt number exhibits a slow gradual rise to a new asymptotic value, which is higher than the constant wall flux case. In case 2, the wall flux rises rapidly from a negative value and passes through zero near $X^* = 0.029$. As the wall flux passes through zero, infinite negative and positive values for the Nusselt number occur. The reason for this anomalous behavior is demonstrated in Figure 9. When $X^* = 0.032$, the temperature gradient at the wall indicates that heat is flowing from the wall, but the average gas temperature T_G^* is higher than T_w^*; thus a large negative value results for the Nusselt number. At $X^* = 0.033$, $(\partial T_G^*/\partial R)_w$ and $(T_w^* - \overline{T}_G^*)$ are both positive, and the heat flow from the wall to the gas is large. Since $(\partial T_G^*/\partial R)_w$ is large relative to $(T_w^* - \overline{T}_G^*)$, a large positive value for the Nusselt number results. Axial gas-phase conduction should not significantly affect this behavior.

The behavior of the Nusselt number as a result of a jump in wall temperature depends on the magnitude of the jump. In Figure 10 the gas enters the tube with $\overline{T}_G^* = 1$ and $T_w^* = 0.0$. At the point $X^* = 0.25$, $\overline{T}_G^*$ is 0.0224. For case 1, T_w^* remains at zero, and the value of the Nusselt number remains constant. For cases 2 and 3 the wall temperature jumps, and new thermal entrance regions are formed. In case 2, the new wall temperature is less than $\overline{T}_G^*$, and the Nusselt number takes on large negative values; in case 3, the new T_w^* is higher than $\overline{T}_G^*$, and the Nusselt number takes on large positive values.

The results of the two-dimensional model also show that the Nusselt number exhibits a spike at the light-off point (Figure 11). Prior to light-off, the Nusselt number is close to the value for the constant wall flux Graetz solution ($Nu = 4.364$) shown as a dotted line in Figure 11 (case 1). At light-off a new entrance region is formed, and the subsequent Nusselt number follows the value for the constant wall temperature Graetz solution ($Nu = 3.657$) which is shown as a dashed line. Similar behavior was demonstrated by Young and Finlayson (1974). The results of the two-dimensional model are qualitatively similar to those of the one-dimensional model. The model exhibits no reaction light-off for low inlet gas temperature (case 1), $T°_G < 293°C$; light-off in the tube for intermediate inlet gas temperatures (case 2 and 3), $293 < T°_G < 343°C$; and light-off at the tube inlet for high inlet gas temperatures (case 4).

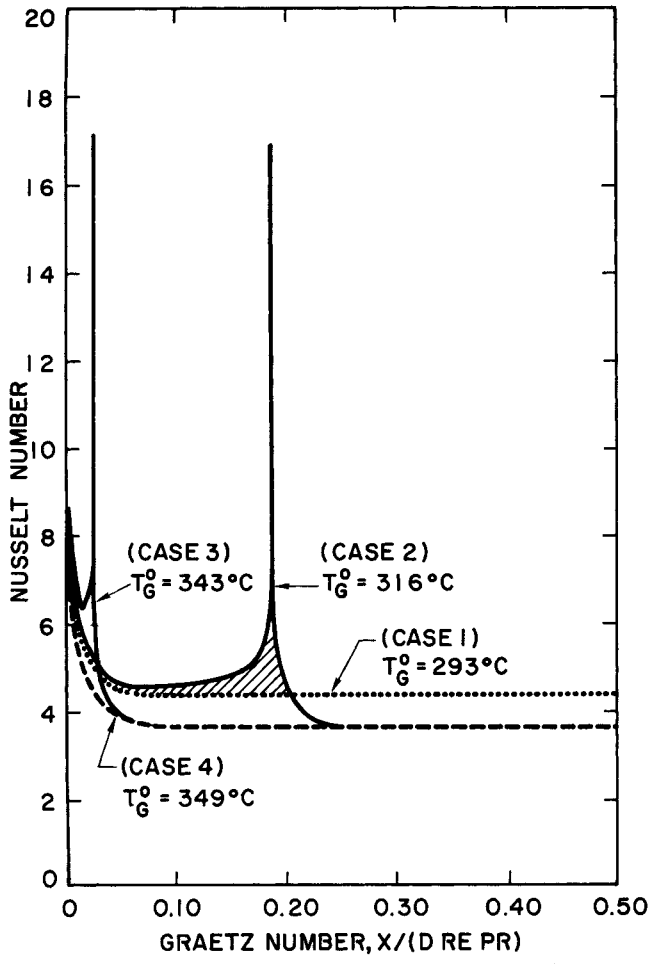

Fig. 11. Nusselt number behavior from two-dimensional reaction model.

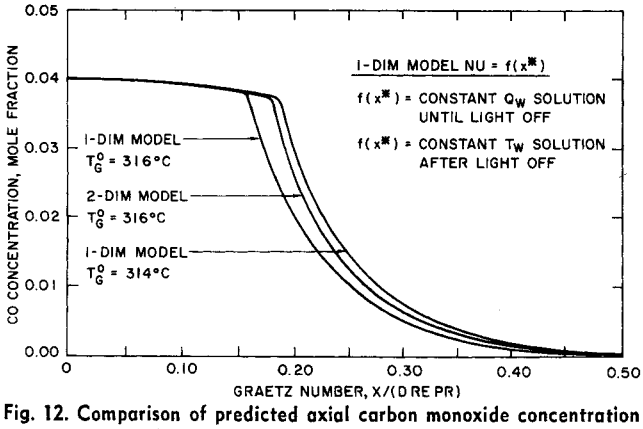

Fig. 12. Comparison of predicted axial carbon monoxide concentration profile from one- and two-dimensional models.

The adequacy of the one-dimensional model depends on the agreement between the conversion predicted by it and that predicted by the two-dimensional model. Figure 12 compares the concentration profiles predicted by the one- and two-dimensional models. For the one-dimensional model, the Nusselt number was assumed to follow the analytical solution for constant wall flux in a cylindrical tube prior to light-off. Once light-off occurred, a new entrance region was assumed, and the analytical solution for constant wall temperature was used for Nu. The analytical solutions of Grigull and Tratz (1965) for constant wall temperature

$$Nu = 3.655 + 6.874\,X^{*-0.488}\exp(-0.0572X^*)$$

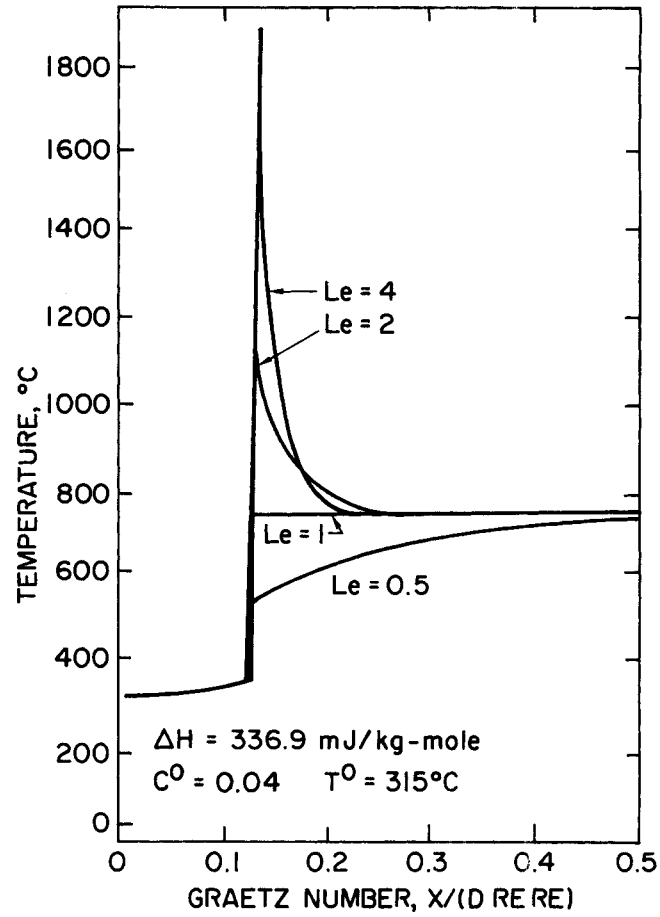

Fig. 13. Effect of Lewis number on wall-temperature profile.

and for constant wall flux

$$Nu = 4.364 + 8.68X^{*-0.506}\exp(-0.041X^*)$$

were used.

Light-off is predicted to occur earlier by the one-dimensional model than by the two-dimensional model because the one-dimensional model slightly underestimates the Nusselt number; lower Nusselt number means earlier light-off (Figure 3). The hatched region in Figure 11 indicates the extent of underestimation in the one-dimensional model. In terms of light-off point and conversion, the difference between the one- and two-dimensional models is equivalent to less than a 2°C difference in inlet gas temperature. When we consider the accuracy to which the inlet gas temperature is known in this system, the deviation between the two models is quite small. In addition, the multiple solutions of the one-dimensional model, exhibited in Figure 1 at the tube inlet, are eliminated by this procedure. Since the one-dimensional model predicts monolith reactor performance very accurately and requires about one-tenth the computing time of the two-dimensional model, it represents the most practical model to use in modeling reactor performance when we consider the critical warm-up period of an automobile from a cold start.

Other Reactants

Thus far it has been assumed that carbon monoxide is the reacting species. Since the Lewis number for carbon monoxide is close to 1.0, the maximum solid temperature is approximately equal to the adiabatic temperature rise at and after light-off. If in Equation (13) we assume that $C_G = C_G^\circ$ and $C_w \cong 0$ at light-off, we see that

$$T_{w,\,\text{light-off}} \cong T_G^\circ + Le\,\Delta T_{AD} \qquad (20)$$

Figure 13 shows the one-dimensional model predictions of the wall temperature profile for $Le = 0.5$, 1, 2, and 4. For molecules with $Le > 1$, the wall temperature can be higher than the adiabatic gas temperature. Hegedus (1975) has shown this overshoot experimentally for the oxidation of hydrogen ($Le \cong 4$); no overshoot was observed for the oxidation of carbon monoxide ($Le \cong 1.0$), and an overshoot was observed for the oxidation of propylene. Inlet mole fraction and heat of reaction were held constant to illustrate the effect of Lewis number; hydrogen mole fraction would typically be lower than 0.04, diminishing the extent of temperature overshoot but not its presence.

Axial Conduction Effects

The effect of axial conduction in either the solid or the gas phase has not been included in the present models owing to the increased difficulty of solving the resultant equations. The importance of axial conduction relative to forced convection will depend on the relative magnitudes of $\partial^2 T_w/\partial x^2$, $\partial^2 T_G/\partial x^2$, and $\partial T_G/\partial R|_w$. Axial conduction in the gas should have little effect and can easily be ignored. In the light-off region, $\partial^2 T_w/\partial x^2 \rightarrow \infty$ (Figure 2). Therefore, in this region axial conduction must be important, and the sharpness of the wall temperature profile will be rounded to more of an S shaped curve.

When conduction is neglected in the monolith models, the front part of the monolith channel is not affected by light-off further down the channel. In reality, light-off would tend to heat the front part of the monolith by conduction and thermal radiation, and the light-off point should move closer to the monolith entrance.

CONCLUSIONS

A simple one-dimensional mathematical model of a catalytic monolith with constant Nusselt number predicts monolith behavior which is quantitatively similar to that predicted by a two-dimensional model in which the Nusselt number is determined from radial gradients. The Nusselt number from the two-dimensional model exhibits very large deviations from the constant asymptotic values in the entrance region and near the light-off point. However, when analytical solutions for the value of the Nusselt number for constant wall flux and constant wall temperature are used, the one-dimensional model predictions are in very good agreement with those of the two-dimensional model. Since the one-dimensional model requires only about one-tenth the computation time of the two-dimensional model, it would appear to be the most practical model to use in predicting the critical warm-up of an automobile from a cold start.

When the Lewis number is one, the behavior of a monolithic reactor is dominated by the position of the light-off point, where wall temperature jumps to the adiabatic flame temperature, and the reaction becomes transport limited. The light-off point depends primarily on the inlet gas temperature and secondarily on channel diameter and geometry. Large Nusselt numbers and small channel diameters lead to better heat transfer and a delay in light-off; this disadvantage is partly offset by a better mass transfer and better conversion in the channel after light-off. When the Lewis number is greater than one, such as for hydrogen, the wall temperature may jump to a value much higher than the adiabatic flame temperature and can contribute to monolith failure.

ACKNOWLEDGMENT

Roland H. Heck was supported by a Mobil Incentive Fellowship.

NOTATION

C = concentration of limiting reactant, typically carbon monoxide, mole fraction
C_{O_2} = concentration of oxygen, mole fraction
C_p = specific heat, joule/kg · °K
D = hydraulic diameter, 4 (cross-sectional area of tube)/(wetted perimeter), m
$\mathcal{D}$ = diffusivity, m^2/s
E = activation energy, joule/kg mole
G = mass flux, kg/m^2 s
h = heat transfer coefficient, joule/m^2 · K · s
ΔH = heat of reaction, joule/kg mole
k_G = thermal conductivity of the gas, joule/m · °K · s
k_a = adsorption coefficient
k_m = mass transfer coefficient, m/s
k_r = rate constant, kg · mole/m^2 · s
Le = Lewis number, $\mathcal{D}\,\rho_G\,C_{PG}/k_G$
M_G = molecular weight of gas, kg/kg mole
Nu = Nusselt number, hD/k_G
Pr = Prandtl number, $C_p\mu/k$
Q = heat flux at wall, joule/m^2 · s
r = rate of reaction, kg mole/m^2 · s
R = dimensionless radial distance
Re = Reynolds number, $DV\rho/\mu$
R_g = gas constant, joule/kg mole · °K
S = surface to volume ratio of channel, m^{-1}
Sh = Sherwood number, $k_M D/\mathcal{D}$
t = time, s
T = temperature, °C
T_G^* = dimensionless gas temperature, $\dfrac{T_G - T_w^\circ}{T_G^\circ - T_w^\circ}$
T_w^* = dimensionless wall temperature, $\dfrac{T_w - T_w^\circ}{T_G^\circ - T_w^\circ}$
$\overline{V}$ = average velocity in channel, m/s
x = axial distance, m
X^* = Graetz number, $4x/(D\,Re\,Pr)$
ρ = density, kg/m^3
μ = viscosity, N · s/m^2

Subscripts

G = gas
w = wall

Superscripts

o = entrance conditions or initial conditions
overbar = integrated average or mixing cup value in two-dimensional model

LITERATURE CITED

Ferguson, N. B., and B. A. Finlayson, "Transient Mathematical Model of a Catalytic Muffler," paper presented at AIChE Natl. Meeting (Nov. 11-15, 1973).

———, "Transient Modeling of a Catalytic Converter to Reduce Nitric Oxide in Automobile Exhaust," *AIChE J.* **20**, 539-550 (1974).

Grigull, V., and H. Tratz, "Thermerscher Einlauf in Ausgebildetu Laminarer Rohrstromung," *Intern. J. Heat Mass Transfer*, **8**, 669 (1965).

Harned, J. L., "Analytical Evaluation of Catalytic Converter Systems," SAE Paper No. 720520, Society of Automotive Engineering, Detroit, Mich. (May, 1973).

Hegedus, L. L., "Temperatures Excursions in Catalytic Monolith," *AIChE J.*, **21**, 899 (1975).

Kays, W. M., "Numerical Solutions for Laminar-Flow Heat Transfer in Circular Tubes," *Trans. Am. Soc. Mech. Engrs.*, **77**, 1265 (1955).

Kuo, J. C., C. R. Morgan, and H. G. Lassen, "Mathematical Modeling of CO and HC Catalytic Converter Systems," *SAE Transactions*, **80**, paper 710289 (1971).

Shar, R. K., and A. L. London, "Laminar Flow Forced Con-

vection Heat Transfer and Flow Friction in Straight and Curved Ducts—a Summary of Analytical Solutions," Stanford University, Department of Mechanical Eng., Stanford, California, *Tech. Rept. No. 75* (Nov. 1, 1971).
Vardi, J., and W. F. Biller, "Thermal Behavior of Exhaust Gas Catalytic Convertor," *Ind. Eng. Chem. Process Design Develop.*, 7, 83 (1968).
Voltz, S. E., C. R. Morgan, D. Liederman, and S. M. Jacob, "Kinetic Study of Carbon Monoxide Oxidation on Platinum Catalysts," *Ind. Eng. Chem. Prod. Res. Develop.*, 12, 295 (1973).
Young, L. C., and B. A. Finlayson, "Mathematical Modeling of the Monolith Converter," in *Advances in Chemistry Series*, R. F. Gould, ed., American Chemical Society, Washington, D.C. (1974).

Manuscript received October 7, 1975; revision received January 16 and accepted January 17, 1976.

Mass Transfer to Drops Moving Through Power Law Fluids in the Intermediate Reynolds Number Region

The mass transfer rate to fluid spheres is calculated for power law and Newtonian fluids by using the intermediate Reynolds number stream functions of Nakano and Tien (1970) and Yamaguchi et al. (1974), respectively. The *Sh* increases with increases in *Re* and *Pe* and decreases in *n*. Better results are obtained with Nakano and Tien's functions when $Re > 10$ and with Yamaguchi's functions when $Re < 10$.

ROBERT M. WELLEK
and
TÜRKER GÜRKAN

Department of Chemical Engineering
University of Missouri-Rolla
Rolla, Missouri 65401

SCOPE

Mass transfer from bubbles and drops is an important and active research area in the field of chemical engineering. Its subject matter has important applications in the design of contacting equipment for processes such as distillation, gas absorption, and liquid-liquid extraction. Large numbers of experimental and theoretical studies have been published on systems in which both phases are Newtonian fluids. However, in recent years the number of physical systems for which the fluid mechanics can only be described by non-Newtonian models has been increasing. The following are examples of industrial processes in which non-Newtonian phases are encountered: activated sludge processes, pharmaceutical production, polymerization processes, lubrication oil production, paint production, and food processing. In order to cope with the problem of estimating mass transfer rates in non-Newtonian systems, a number of researchers have recently focused their efforts on non-Newtonian dispersed phase phenomena.

Gürkan and Wellek (1976) numerically solved the diffusion equation for the creeping flow of a Newtonian droplet in a power law type of fluid by using the Mohan (1974) stream functions. Nakano and Tien (1970) have presented a set of stream functions for a drop moving through a power law type of fluid in the intermediate Reynolds number region. Experimental liquid-liquid extraction data have been presented by Schafermeyer et al. (1975) for the case of mass transfer to a droplet from a non-Newtonian continuous phase when the resistance to mass transfer is in the continuous phase. Yamaguchi et al. (1974) proposed a new set of stream functions, the use of which enabled them to predict droplet drag and continuous phase mass transfer coefficients with a smooth transition from the creeping flow regime to the intermediate Reynolds number region; their analysis involved only Newtonian fluids. However, we believe their type of stream functions may prove useful for the study of non-Newtonian fluid flow around drops. Because the Reynolds numbers encountered in droplet phenomena often fall into the range of the intermediate Reynolds number region, the prediction of the rate of mass transfer in this region for both Newtonian and non-Newtonian fluids is important and is, therefore, the subject of the current investigation.

The specific objectives of the present study are: to quantitatively predict the continuous phase Sherwood number for a Newtonian droplet moving through a power law type of continuous phase in the intermediate Reynolds number region, to determine the effect of the Reynolds number and the power law flow behavior index on the Sherwood number in the intermediate Reynolds number region, and to compare the theoretical results, which are obtained by using the Nakano and Tien (1970) and the Yamaguchi et al. (1974) types of stream functions, with available experimental data.

CONCLUSIONS AND SIGNIFICANCE

The results obtained from the solution of the mathematical model show that in the intermediate Reynolds number region, the continuous phase Sherwood number increases with a decrease in the flow behavior index *n* and with an increase in the Reynolds and the Peclet numbers for flow through a power law fluid. The mass transfer results obtained in this study by using the Nakano and Tien (1970) stream functions do not converge, as the Reynolds number is decreased, with the results of Gürkan and Wellek (1976) which were developed by using the

Correspondence concerning this paper should be addressed to Robert M. Wellek.